

Connecting DUNE to UV models through an EFT pipeline

Adriano Cherchiglia^a

^a*Instituto de Física Gleb Wataghin, Universidade Estadual de Campinas, Rua Sérgio Buarque de Holanda, 777, Campinas, 13083-859, Sao Paulo, Brazil*

Abstract

Future neutrino experiments, in particular DUNE, are expected to probe signals of new physics. Those can be conveniently parametrized in terms of Wilson coefficients in the LEFT, with direct connection to non-standard interactions at production, propagation and detection in the QFT formalism. Assuming that the new degrees of freedom lie above the electroweak scale, we investigate if a DUNE-motivated signal, described by a non-vanishing SMEFT Wilson coefficient, can be realized in UV completions containing extra isosinglet and/or isodoublet fields, once present flavour constraints are taken into account. To this end, we propose a pipeline which can, in principle, be applicable to any BSM signal parametrized by a given set of SMEFT Wilson coefficients. As a concrete example, we focus on the lepton-flavour-violating semileptonic coefficient ($C_{\ell q,1311}^{(1)}$). We find that the largest viable value of the target Wilson coefficient remains around (10^{-2} TeV⁻²), which is almost one order of magnitude below the DUNE benchmark.

Keywords: Effective Field Theories, Neutrinos, Beyond the Standard Model

1. Introduction

The discovery of neutrino oscillations established that lepton flavour is not an exact symmetry of Nature and provided one of the clearest indications that the Standard Model (SM), in its minimal form, is incomplete. The next generation of long-baseline neutrino experiments, and in particular DUNE, will test the three-neutrino paradigm with unprecedented precision and will be sensitive to subleading effects that may arise from new physics in neutrino production, propagation or detection [1–4]. Such effects are usually parametrized as non-standard interactions (NSI) [5–8], which, in the QFT approach, are directly connected to effective field theories [9–28].

Regarding UV completions, one can connect NSIs to all possible weakly coupled states, with masses above the electroweak scale and subjected to the SM gauge group. This map is possible due to the existence of SMEFT dictionaries both at tree-level [29], and one-loop [30, 31]. In [32], we have shown how this idea, at tree-level matching, can be automatically implemented. Partial extensions to one-loop matching were also put forward [33].

Recently, a comprehensive analysis of DUNE sensitivity to SMEFT Wilson coefficients (WC) was done [27]. Although present bounds on the majority of the WCs are stronger than DUNE capabilities, the semileptonic coefficient, $C_{\ell q,1311}^{(1)}$, deserves more attention, since it is still not very strongly constrained. For instance, performing an analysis with `sme11i` [34–36], one can extract bounds of order 10^{-1} TeV⁻², weaker than DUNE prospects, while other global fits obtain bounds one order of magnitude stronger [37]. In view of this scenario, in this work we will perform the following exercise: given a target value for $C_{\ell q,1311}^{(1)}$, how large can this coefficient become in weakly coupled UV completion, once flavour con-

straints are imposed? In order to answer this question, we propose a pipeline to systematically survey the space of UV models. Although it may be seen as an exercise at present, the driving idea is to set the stage once an anomaly at DUNE (or elsewhere) is clearly characterized as a given SMEFT WC. In particular, we first perform a broad scan over UV completions and then focus on the most promising model, studying both the full parameter space and sparse subsets of couplings. This allows us not only to determine the largest viable value of the target coefficient, but also to identify which interactions are responsible for generating it.

Our main result is that, within the class of UV completions considered here, the maximal viable value of $C_{\ell q,1311}^{(1)}$ is almost one order of magnitude lower than the sensitivity of DUNE. Although it may not be seen as a no-go result in general, for the usual BSM models, based on new scalars and/or fermions at representations up to doublets under SU(2)_L, we could not find any viable candidate. Thus, if the DUNE simulated result was indeed an anomaly, more exotic UV completions would need to be invoked. Our work is organized as follows: in section 2 we propose our pipeline, finding the best UV model candidate, while in section 3 we scrutinize the best model in more detail. We conclude in section 4.

2. Seeking for UV completions

In this section we describe the main goal of our work, which aims to answer the following question: given that DUNE reports an anomaly in one of the SMEFT WC, which UV model can be behind it? We will be using DUNE as example throughout our work, however, the pipeline proposed here can be applied to any other experiment in principle.

Since DUNE is not even operating yet, we will rely on simulations to extract its sensitivity to SMEFT WCs, using the comprehensive analysis done in [27]. In general, non-diagonal SMEFT WC related to fermions are very constrained, due to the non-observation of charged lepton flavour violation signals. Thus, when seeking for UV models, only diagonal ones were considered in [32]. In this work, we lift this assumption. We will look in particular at $C_{\ell q}^{(1)}$, that is still less constrained at present [37]. We recall that this SMEFT WC is related to the following dimension-six SMEFT operator

$$\mathcal{O}_{\ell q}^{(1)} = (\bar{\ell}_\alpha \gamma_\mu \ell_\beta)(\bar{q}_i \gamma^\mu q_j). \quad (1)$$

As we collected in [32], there is a connection between NSI at propagation and SMEFT WC. For Earth-based neutrino experiments, such as DUNE, one obtains for the case that only $C_{\ell q}^{(1)}$ is non-zero

$$\epsilon_{\alpha\beta} = -2v^2 C_{\ell q}^{(1)}{}_{\alpha\beta 11}, \quad (2)$$

where, for simplicity, we adopt a diagonal CKM in the above formula. We recall that the presence of $\epsilon_{\alpha\beta}$ modifies the propagation of neutrinos through matter. In particular, if ϵ_{13} ($\epsilon_{e\tau}$) is non-null, it implies mainly on a modification of the number of events predicted in the (anti)electron appearance channels at DUNE.

From [27], we extract the bound at 90% C.L., for one non-null SMEFT at a time, as

$$C_{\ell q}^{(1)}{}_{1311} < 9 \times 10^{-2} \text{ TeV}^{-2}, \quad (3)$$

which corresponds to $\epsilon_{e\tau} < 0.012$, stronger than the bound found, for instance, in [38].

In this work we will suppose that, after seven years of data collection at DUNE, an anomaly is reported which amounts to a best-fit value of $C_{\ell q}^{(1)}{}_{1311} = 9 \times 10^{-2} \text{ TeV}^{-2}$. This assumption is probably too optimistic, since the analysis would probably point to other SMEFT WC being non-null as well, which would deteriorate the expected sensitivity on $C_{\ell q}^{(1)}$. Since the experiment is not running yet, we can consider this optimistic scenario, which can be seen as an exercise for a true reported anomaly in the future. For definiteness, we will denote the SMEFT WC that contains the anomaly as the C_{target} . In the following, we will describe our general approach to seek UV models.

Our starting point is to find, using the C_{target} as guide, which UV models can generate it. To this end, we employ the tool SOLD [30, 31], whose main aim is exactly to provide dictionaries for SMEFT WCs. We will adopt one-loop matching, considering new fermions and/or scalars, as usual assumed in BSM phenomenology. Since our target EFT is the SMEFT, we are implicitly assuming that all BSM states are heavy (in our numerical evaluations we will set all masses at 1 TeV for definiteness). By employing SOLD, we find a total of 338 possible UV models. In order to reduce the set, we will restrict ourselves only to isosinglets and/or isodoublets (a common choice

in most of BSM models), which gives us a total of 112 UV models. Once the set is established, we proceed to obtain the matching (up to one-loop) to the SMEFT for each of the 112 models. This step is essential, since a given model will not only generate the C_{target} , but potentially many other WCs which can be heavily constrained.

For each UV scenario, its WCs will be functions of the models parameters, which we will denote generically as θ_j . Thus, for each UV model we obtain a set of non-null SMEFT WC of the form $C_i(\theta_j)$. Once their analytic expression is known, we proceed to find the most promising candidates that maximize the C_{target} still complying with present constraints. This task is very complex in general, since the UV models found can contain up to four mediators. Moreover, since no extra symmetry is assumed (on top of the SM gauge group), the BSM mediators can couple in many different ways among themselves and among the SM particles. Since our C_{target} does not contain indexes on the second family, we will adopt as simplifying assumption that the BSM states do not couple to the second lepton family (muonphobic couplings), reducing the number of free parameter. We also set to zero all the free parameters that do not appear on C_{target} . Nevertheless, even under these simplifying assumptions, performing a global fit in the multi-dimensional parameter space of each of the 112 UV models is unfeasible. Thus, we will first adopt a simplified approach to the problem in order to reduce the number of promising models.

In [39] the present bounds on a large set of SMEFT WCs is presented, both from a global fit as well as for individual coefficients. In a first stage we take the limits for the individual coefficients as our bounds since they provide a fast estimate of which regions of the UV parameter space can potentially generate a sizeable target coefficient without immediately producing other excluded SMEFT WCs. In this first step, the constraints are imposed as

$$|C_i(\theta)| \leq B_i, \quad (4)$$

where B_i is the corresponding bound from [39]¹, and we also enforce perturbativity by setting $|\theta_i| \leq 1$.

First, for each UV model, we perform a Monte Carlo sampling (around 10^6 points) on its parameter space, ranking each solution by the value of the C_{target} achieved subjected to the constraints of eq.4. From those solutions, we built 12 clusters from the top 10% solutions, to which we perform a numerical optimization to the target coefficient while satisfying the remaining bounds. We emphasize that this preliminary stage is used only to identify promising UV models and seed points. The main result of this first stage is the possibility to sort the UV models that can maximize the C_{target} , as well as obtain the point on the UV parameter space responsible for this feature, which we will denote as seed. We obtain, after the completion of the first stage, that a still large set of models can attain $|C_i(\theta)| \sim 4.5 \times 10^{-3} \text{ TeV}^{-2}$.

¹We choose to consider the bounds from the $U(2)^5$ case at 1 TeV, which is the case with the most number of WCs. The 1 TeV is for consistency with the scale of our mediators.

Once the seed is known, we move to the second stage, where we employ `flavio` [34], `wilson` [35], and `smelli` [36] to obtain the global likelihood for the seed, $\chi^2(\theta_{\text{seed}})$. Considering the SM scenario, $\chi^2(\theta_i = 0)$, as the best-fit, for some of the UV models their seeds give a very large $\Delta\chi^2$. This feature is somewhat expected since the set of observables implemented in `flavio` is larger than those considered in [39]. Given this result, we remove from our set of promising models those for which $\Delta\chi^2 > 700$, obtaining 24 UV models.

Our next task is to survey the 24 remaining candidates more thoroughly. To this end, starting from the seed, we implement a constrained optimization problem where we maximize $C_{\text{target}}(\theta)$ subject to

$$\chi^2(\theta) \leq \chi_{\text{SM}}^2 + \Delta\chi_{\text{max}}^2, \quad |\theta_i| \leq 1. \quad (5)$$

Here χ_{SM}^2 is the value of the likelihood at the Standard Model point, while $\Delta\chi_{\text{max}}^2$ specifies the tolerated degradation of the global fit. Unless otherwise stated, we use

$$\Delta\chi_{\text{max}}^2 = 4, \quad (6)$$

which provides a conservative criterion for retaining points close to the global Standard Model fit. This value is also chosen to somewhat penalize models with many parameters, since $\Delta\chi^2 = 4$ represents a 2 sigma deviation for a one-parameter UV model, while for more free parameters the number of sigma deviations is smaller. We obtain that the second stage allows an improvement of 17 of the 24 UV models, as can be seen on table 1. For further reference, we found $\chi_{\text{SM}}^2 = 747$. It is interesting to notice that for most of the models the optimization step with `smelli` does not alter the χ^2 significantly. The main exceptions are models 289, 288, 296 which started with a large χ^2 in the seed evaluation, however, the optimization step not only found a better point but also increased the value of C_{target} . For other models such as 95 (and others not collected in the table), the starting χ^2 is large and the optimization step can decrease it with the expense of also decreasing the value of the C_{target} .

At this stage we can already answer the question posed in the beginning of the section. If DUNE does indeed report an anomaly as given in eq. 3, we could not find any viable UV model that can reach this signal. Our best candidate can reach up to 16% of the C_{target} , still complying with present bounds from flavour.

In the next section we will scrutinize further our best candidate. We end this section with a brief summary of our approach that is in principle general for seeking UV models for any anomaly reported as SMEFT WC. The overall strategy was to separate the problem into three levels. First, we identified the models at one-loop matching that could give the C_{target} employing UV dictionaries. Second, approximate SMEFT bounds were used to identify UV models capable of generating a potentially observable signal. Third, the full flavour likelihood is used to find if such points survive a larger set of precision constraints, as well as to optimize the search for the maximal C_{target} in a given model.

Table 1: Set of promising models surveyed. The column $C_{\text{target}}^{\text{seed}}$ gives the target coefficient before the optimization step (`smelli`-based optimization), while $C_{\text{target}}^{\text{opt}}$ is the value found after this step.

Model	$C_{\text{target}}^{\text{seed}}$ (TeV ⁻²)	χ_{seed}^2	χ_{opt}^2	$C_{\text{target}}^{\text{opt}}$ (TeV ⁻²)
289	4.49×10^{-3}	832.4	750.2	1.49×10^{-2}
291	4.46×10^{-3}	749.6	752.4	1.25×10^{-2}
336	4.45×10^{-3}	746.7	747.3	1.09×10^{-2}
106	4.12×10^{-3}	749.5	748.3	1.02×10^{-2}
335	4.48×10^{-3}	747.5	743.5	9.05×10^{-3}
331	4.48×10^{-3}	747.8	752.0	8.38×10^{-3}
165	4.49×10^{-3}	749.0	750.4	8.27×10^{-3}
169	4.49×10^{-3}	749.7	749.6	8.22×10^{-3}
102	4.42×10^{-3}	748.4	750.2	8.08×10^{-3}
332	4.45×10^{-3}	744.5	751.4	8.05×10^{-3}
104	4.49×10^{-3}	751.3	750.8	8.12×10^{-3}
288	4.49×10^{-3}	969.7	747.0	7.72×10^{-3}
21	4.49×10^{-3}	749.8	750.4	7.71×10^{-3}
96	4.49×10^{-3}	747.5	747.7	7.69×10^{-3}
286	4.43×10^{-3}	759.0	749.1	7.48×10^{-3}
296	4.43×10^{-3}	964.6	738.7	7.02×10^{-3}
105	4.49×10^{-3}	756.9	751.1	6.69×10^{-3}
27	4.47×10^{-3}	747.8	751.2	4.47×10^{-3}
100	4.49×10^{-3}	756.3	754.8	4.49×10^{-3}
98	4.41×10^{-3}	748.1	749.7	4.41×10^{-3}
99	4.35×10^{-3}	789.6	748.8	2.32×10^{-3}
95	4.49×10^{-3}	1511	750.5	2.28×10^{-4}

3. Scrutinizing the best UV model

In the last section we found that the best UV model to maximize C_{target} still complying with present constraints is model 289. The number itself is irrelevant, it is just a label to organize the 338 possible UV models that can, in principle, generate $C_{\ell q}^{(1)}$. In this section we will scrutinize it further.

We begin with a definition of the BSM fields added. This model contains a scalar field, denoted here by S , and vector-like fermionic fields, denoted by F_a and F_b (in the notation of [29], those are ω_1 , E^c , U respectively). Schematically, the interactions relevant for the generation of the semileptonic operator, $C_{\ell q}^{(1)}$, take the form

$$\mathcal{L}_{\text{int}} \supset \lambda_{\ell q}^S S^\dagger \bar{q}_L i\sigma_2 \ell_L + \lambda_{\phi q}^{F_b} \bar{F}_{bR} \bar{\phi}^\dagger q_L + \lambda_{\phi \ell}^{F_a} \bar{F}_{aR} \phi^\dagger \ell_L + \text{h.c.} \quad (7)$$

where the quantum numbers of the BSM states are organized on table 2. The SM fields are denoted as usual: q, ℓ, ϕ for the quark, lepton, and Higgs doublets.

Table 2: New fields entering the representative benchmark model.

Field	Spin	$SU(3)_c$	$SU(2)_L$	$U(1)_Y$
S	0	3	1	-1/3
F_a	1/2	1	1	1
F_b	1/2	3	1	2/3

The direct coupling of S to the leptonic and quark doublets generates semileptonic four-fermion operators after the heavy scalar is integrated out (tree-level matching). In particular, one

obtains correlated contributions to

$$\mathcal{O}_{\ell q}^{(1)} = (\bar{\ell}_L \gamma_\mu \ell_L)(\bar{q}_L \gamma^\mu q_L) \quad (8)$$

and

$$\mathcal{O}_{\ell q}^{(3)} = (\bar{\ell}_L \gamma_\mu \tau^I \ell_L)(\bar{q}_L \gamma^\mu \tau^I q_L). \quad (9)$$

Explicitly, at tree-level matching, we obtain

$$C_{\ell q}^{(1)} = -C_{\ell q}^{(3)} = \frac{(\lambda_{\ell q}^{S^\dagger})_{\alpha i} (\lambda_{\ell q}^S)_{\beta j}}{4M_S^2}. \quad (10)$$

Notice that, at tree-level, only the scalar is relevant. As we are going to see, eq.10 will be responsible for the most part of the contribution to C_{target} . Nevertheless, in our analysis we use the one-loop matching full contribution, whose expression is lengthy. So we refrain from presenting it here.

We found that C_{target} is maximized when 16 free parameters are non-null. An immediate problem is the occurrence of couplings connecting the quark doublet and lepton doublet as well as only quark doublets. This will generate, in general, very dangerous baryon-violating operators that are heavily suppressed. We have checked our best model candidates and found that a similar issue happens for the vast majority. Therefore, the results in table 1 are to be interpreted in terms of optimistic candidates subjected mainly to flavour observables implemented in the global fit used here. In any case, our conclusion remains: it seems not to be feasible to obtain a UV model capable of explaining an anomaly on the C_{target} reported by DUNE.

Nevertheless, we checked that model 289 still constitutes a good candidate when couplings λ_{qq}^S are null, performing the entire optimization once more under this new constraint. We found that $C_{\text{target}} = 1.32 \times 10^{-2} \text{ TeV}^{-2}$, which is only a reduction of around 10%, making it still the best candidate model. We will quote, hereafter, this value as the C_{target} maximal value for model 289. We collect the values of the best-fit parameters in table 3.

Table 3: Values of the free parameters of model 289 when maximizing the target coefficient.

Free parameter	Value
$\lambda_{\phi q}^{F_b}$	{-0.36, 0, 0.089}
$\lambda_{S e}^{F_b}$	{0.45, 0, -0.46}
$\lambda_{\ell q}^S$	$\begin{pmatrix} -0.17 & 0 & -0.31 \\ 0 & 0 & 0 \\ 0 & 0 & 0.06 \end{pmatrix}$
$\lambda_{S d}^{F_b}$	{0.28, 0, -0.089}
$\lambda_{\phi \ell}^{F_a}$	{0.13, 0, 0.17}
$\lambda_{S u}^{F_a}$	{0.35, 0, -0.61}

Another aspect is that, by employing eq.10, we obtain that the tree-level matching formula corresponds to $C_{\text{target}} \sim 1.31 \times$

10^{-2} TeV^{-2} , which is 99% of the maximal value we found. In view of this result, it seems that the 289 model is overcomplicated, since the vector-like fermions play a secondary role. We will see that this is not entirely true, as we will discuss in the next subsection a simplified approach to minimal models which also avoid dangerous baryon-violating operators.

3.1. Minimal UV realization

In this section we will scrutinize minimal realizations based on model 289. Starting from the proton decay bound, we require that couplings λ_{qq}^S are null. In order to do this systematically, we define a support \mathcal{S}_p (minimal set of UV free parameters for non-null C_{target}), while setting all other parameters to zero. We found three sets of supports: $\{(\lambda_{\ell q}^S)_{11}, (\lambda_{\ell q}^S)_{13}\}$; $\{(\lambda_{\ell q}^S)_{13}, (\lambda_{\ell q}^S)_{33}\}$; $\{(\lambda_{\phi \ell}^{F_a})_1, (\lambda_{\phi \ell}^{F_a})_3\}$. The first is just the tree-level contribution, while the other two are one-loop corrections involving emission of $q\bar{q}$ through B_μ or the Higgs (recall we are performing the matching at the unbroken phase of the SMEFT).

Once we have the supports, we then require the reduced point to satisfy the same likelihood condition,

$$\chi^2(\theta_S) \leq \chi_{\text{SM}}^2 + \Delta\chi_{\text{max}}^2, \quad (11)$$

while optimizing the $C_{\text{target}}(\theta_{\mathcal{S}_p})$. Unsurprisingly, only the first support will give a sizable contribution. However, we find $C_{\text{target}} = 7.66 \times 10^{-3} \text{ TeV}^{-2}$, which is only 58% of the previous C_{target} with 13 free parameters.

Since we have now only two free parameters, it is feasible to obtain two-dimensional likelihood profiles, which we depict in figure 1. We also show in the heatmap the value of the C_{target} . We only show the support $\{(\lambda_{\ell q}^S)_{11}, (\lambda_{\ell q}^S)_{13}\}$, since the other two cannot produce any sizable contributions.

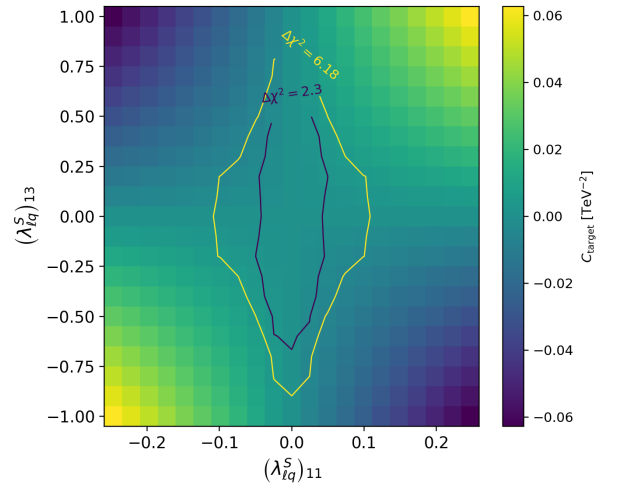


Figure 1: Profile likelihood in the two-parameter support $\{(\lambda_{\ell q}^S)_{11}, (\lambda_{\ell q}^S)_{13}\}$. The heatmap shows the value of the target coefficient, $C_{\ell q,1311}^{(1)}$. We also depict $1(2)\sigma$ C.L. in blue (yellow). All remaining UV parameters are set to zero.

We proceed now to consider the case where 3 parameters are non-null. In this scenario, there is a total of 14 supports. We

found that the support $\{(\lambda_{lq}^S)_{11}, (\lambda_{lq}^S)_{13}, (\lambda_{\phi q}^{F_b})_1\}$ gives the largest contribution. We now obtain $C_{\text{target}} = 9.52 \times 10^{-3} \text{ TeV}^{-2}$, which is 72% of the previous C_{target} with 13 free parameters. It is interesting to notice that for this model, on top of λ_{lq}^S , we have the couplings to the fermion F_b given by $\lambda_{\phi q}^{F_b}$. Thus, it starts to indicate the importance of enlarging the field content of the UV model. Once again we can obtain likelihood profiles. After marginalization of $(\lambda_{\phi q}^{F_b})_1$, we obtain figure 2, which should be compared with figure 1. Notice that the effect of the inclusion of $(\lambda_{\phi q}^{F_b})_1$ is to enlarge the allowed values for $(\lambda_{lq}^S)_{11}$.

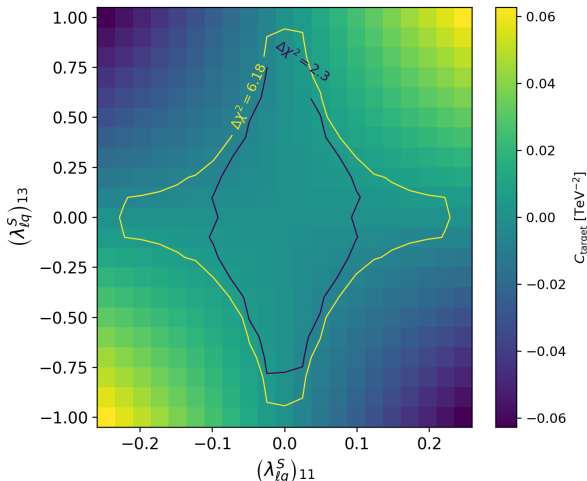


Figure 2: Profile likelihood in the two-parameter support $\{(\lambda_{lq}^S)_{11}, (\lambda_{lq}^S)_{13}\}$. The heat map shows the value of the target coefficient, $C_{lq,1311}^{(1)}$. We also depict $1(2)\sigma$ C.L. in blue (yellow). The parameter $(\lambda_{\phi q}^{F_b})_1$ is marginalized over while all remaining UV parameters are set to zero.

In order to understand better how the inclusion of the coupling $\lambda_{\phi q}^{F_b}$ helps to enlarge C_{target} , we show in figure 3 the 14 largest SMEFT WC generated by each of the cases: full model (13 non-null parameters), only two non-null parameters ($k = 2$), only three non-null parameters ($k = 3$). It is interesting to notice that the WC are generated with similar strength across the different cases.

In figure 3 we also depict the bounds for non-null WC one-at-time as black lines at 90% C.L. These bounds were obtained employing `smelli`, for consistency with our analysis. For $C_{lq,3311}^{(1)}$ the bound is not shown because it is too weak. It is interesting to notice that our C_{target} is poorly constrained. There are, however, other global fits in the literature, the most recent being done in [37]. Using this reference, one obtains the bound

$$C_{lq,1311}^{(1)} < 1.4 \times 10^{-2} \text{ TeV}^{-2}, \quad (12)$$

which is of the order of the maximum C_{target} we found.

Another interesting feature of figure 3 is that the case $k = 3$ generates the same WCs as in the case $k = 2$ with larger values as well as two new WC, $C_{\phi q,11}^{(1,3)}$. The main importance of the last two WC is to create new correlations in the global fit for $k = 3$, which allows $(\lambda_{ql}^S)_{13}$ to increase with respect to the $k = 2$

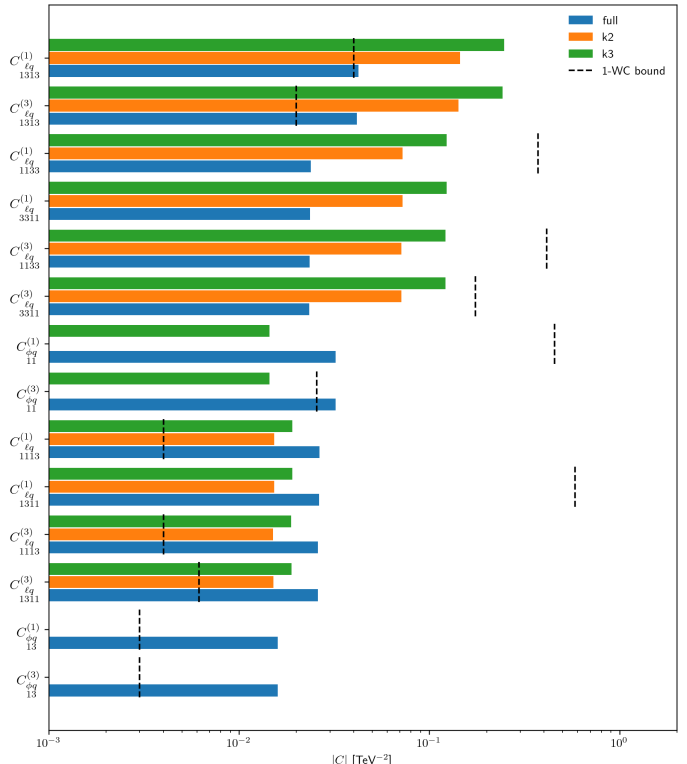


Figure 3: Largest SMEFT Wilson coefficients generated at the benchmark points obtained in the full scan, in the two-parameter support ($k = 2$), and in the three-parameter support ($k = 3$). The vertical dashed lines indicate the corresponding one-Wilson-coefficient-at-a-time bounds obtained with `smelli` at 90% C.L.

case. This feature can be more clearly seen in figure 4 where we show the values for the 13 free parameters for the cases $k = 2, 3$ and full ($k = 13$). As we already mentioned, the tree-level contribution requires the presence of the couplings λ_{lq}^S where the product of the couplings seem to systematically increase as we add more free parameters.

To conclude this section we briefly discuss the approach to find other minimal UV realizations. For two parameters, we have performed a systematic survey, considering all possible supports. Already for three parameters we have adopted a few simplifications, since the number of possibilities starts to increase substantially (recall that for each support a optimization algorithm employing a global fit is triggered). Before employing the optimization stage, we have surveyed the C_{target} into a given support up to perturbativity bounds. If the maximum value found for C_{target} is less than 85% of the maximal value for the full case, we discarded that support².

For the next case, $k=4$, we performed only a partial survey finding a maximal $C_{\text{target}} = 1.03 \times 10^{-2} \text{ TeV}^{-2}$. It corresponds to an improvement of 10% over the case $k = 3$, consisting of around 77% of the maximum value found on the model with 13 non-null parameters. Still, only a vector-like quark is included, now with non-null couplings to the third generation as well.

²For $k = 3$ only three models were removed. We have explicitly checked that they indeed cannot generate any sizable C_{target} .

- [15] A. Falkowski, M. González-Alonso and Z. Tabrizi, *Reactor neutrino oscillations as constraints on Effective Field Theory*, *JHEP* **05** (2019) 173 [1901.04553].
- [16] K.S. Babu, P.S.B. Dev, S. Jana and A. Thapa, *Non-Standard Interactions in Radiative Neutrino Mass Models*, *JHEP* **03** (2020) 006 [1907.09498].
- [17] I. Bischer and W. Rodejohann, *General neutrino interactions from an effective field theory perspective*, *Nucl. Phys. B* **947** (2019) 114746 [1905.08699].
- [18] S. Davidson and M. Gorbahn, *Charged lepton flavor change and nonstandard neutrino interactions*, *Phys. Rev. D* **101** (2020) 015010 [1909.07406].
- [19] J. Terol-Calvo, M. Tórtola and A. Vicente, *High-energy constraints from low-energy neutrino nonstandard interactions*, *Phys. Rev. D* **101** (2020) 095010 [1912.09131].
- [20] K.S. Babu, D. Gonçalves, S. Jana and P.A.N. Machado, *Neutrino Non-Standard Interactions: Complementarity Between LHC and Oscillation Experiments*, *Phys. Lett. B* **815** (2021) 136131 [2003.03383].
- [21] Y. Du, H.-L. Li, J. Tang, S. Vihonen and J.-H. Yu, *Non-standard interactions in SMEFT confronted with terrestrial neutrino experiments*, *JHEP* **03** (2021) 019 [2011.14292].
- [22] A. Falkowski, M. González-Alonso, J. Kopp, Y. Soreq and Z. Tabrizi, *EFT at FASER ν* , *JHEP* **10** (2021) 086 [2105.12136].
- [23] Y. Du, H.-L. Li, J. Tang, S. Vihonen and J.-H. Yu, *Exploring SMEFT induced nonstandard interactions: From COHERENT to neutrino oscillations*, *Phys. Rev. D* **105** (2022) 075022 [2106.15800].
- [24] V. Bresó-Pla, A. Falkowski, M. González-Alonso and K. Monsálvez-Pozo, *EFT analysis of New Physics at COHERENT*, *JHEP* **05** (2023) 074 [2301.07036].
- [25] P. Coloma, E. Fernández-Martínez, J. López-Pavón, X. Marcano, D. Naredo-Tuero and S. Urrea, *Improving the global SMEFT picture with bounds on neutrino NSI*, *JHEP* **02** (2025) 137 [2411.00090].
- [26] J. Kopp, N. Rocco and Z. Tabrizi, *Unleashing the power of EFT in neutrino-nucleus scattering*, *JHEP* **08** (2024) 187 [2401.07902].
- [27] J. Kopp, Z. Tabrizi and S. Urrea, *Effective field theory in long-baseline neutrino oscillation experiments*, *JHEP* **02** (2026) 176 [2509.21537].
- [28] M. González-Alonso, A. Palavrić and S. Prakash, *EFT for Neutrino Oscillations: Theory Developments and Application to JUNO*, 2606.11298.
- [29] J. de Blas, J.C. Criado, M. Perez-Victoria and J. Santiago, *Effective description of general extensions of the Standard Model: the complete tree-level dictionary*, *JHEP* **03** (2018) 109 [1711.10391].
- [30] G. Guedes, P. Olgoso and J. Santiago, *Towards the one loop IR/UV dictionary in the SMEFT: One loop generated operators from new scalars and fermions*, *SciPost Phys.* **15** (2023) 143 [2303.16965].
- [31] G. Guedes and P. Olgoso, *From the EFT to the UV: the complete SMEFT one-loop dictionary*, 2412.14253.
- [32] A. Cherchiglia and J. Santiago, *DUNE potential as a new physics probe*, *JHEP* **03** (2024) 018 [2309.15924].
- [33] A. Cherchiglia, *Unveiling New Physics Models Through Meson Decays and Their Impact on Neutrino Experiments*, *Universe* **11** (2025) 225.
- [34] D.M. Straub, *flavio: a Python package for flavour and precision phenomenology in the Standard Model and beyond*, 1810.08132.
- [35] J. Aebischer, J. Kumar and D.M. Straub, *Wilson: a Python package for the running and matching of Wilson coefficients above and below the electroweak scale*, *Eur. Phys. J. C* **78** (2018) 1026 [1804.05033].
- [36] J. Aebischer, J. Kumar, P. Stangl and D.M. Straub, *A Global Likelihood for Precision Constraints and Flavour Anomalies*, *Eur. Phys. J. C* **79** (2019) 509 [1810.07698].
- [37] E. Fernández-Martínez, X. Marcano and D. Naredo-Tuero, *Global lepton flavour violating constraints on new physics*, *Eur. Phys. J. C* **84** (2024) 666 [2403.09772].
- [38] P. Coloma, M.C. Gonzalez-Garcia, M. Maltoni, J.P. Pinheiro and S. Urrea, *Global constraints on non-standard neutrino interactions with quarks and electrons*, *JHEP* **08** (2023) 032 [2305.07698].
- [39] J. de Blas, A. Gonçalves, V. Miralles, L. Reina, L. Silvestrini and M. Valli, *Constraining new physics effective interactions via a global fit of electroweak, Drell-Yan, Higgs, top, and flavour observables*, *JHEP* **03** (2026) 013 [2507.06191].